

Electron Removal Self Energy and Its Application to $\text{Ca}_2\text{CuO}_2\text{Cl}_2$

Chul Kim¹, S. R. Park¹, C. S. Leem¹, D. J. Song¹, H. U. Jin¹, H.-D. Kim², F. Ronning³ and C. Kim^{1,*}

¹*Institute of Physics and Applied Physics, Yonsei University, Seoul 120-749, Korea*

²*Beamline Research Division, Pohang Accelerator Laboratory,*

POSTECH, Pohang, Kyungbuk 790-784, Korea and

³*MPA-10 Division, Los Alamos National Laboratory, Los Alamos, New Mexico 87545*

(Dated: April 19, 2009)

We propose using the self energy defined for the electron removal Green's function. Starting from the electron removal Green's function, we obtained expressions for the removal self energy $\Sigma^{ER}(\mathbf{k}, \omega)$ that are applicable for non-quasiparticle photoemission spectral functions from a single band system. Our method does not assume momentum independence and produces the self energy in the full $\mathbf{k}-\omega$ space. The method is applied to the angle resolved photoemission from $\text{Ca}_2\text{CuO}_2\text{Cl}_2$ and the result is found to be compatible with the self energy value from the peak width of sharp features. The self energy is found to be only weakly \mathbf{k} -dependent. In addition, the $\text{Im}\Sigma$ shows a maximum at around 1 eV where the high energy kink is located.

PACS numbers: 74.72.-h, 74.25.Jb, 78.20.Bh, 79.60.-i

I. INTRODUCTION

Photoemission lineshape contains information on the many-body interactions in the solid under study. One notable example is the kink structure in the angle resolved photoemission(ARPES) spectral function from a metal at the bosonic mode energy due to electron-bosonic mode coupling^{1,2,3}. In this regard, the kink structures at near 70 meV found in the ARPES spectral functions from cuprate high temperature superconductors (HTSCs) have been a hot topic during the last several years as it may provide a clue on what mediates the pairing in the HTSC^{4,5,6,7,8}. It is still under debate whether the kink is caused by phonons or magnetic excitations. In addition to the kink near 70meV, an anomalous high energy kink structure from insulating cuprate $\text{Ca}_2\text{CuO}_2\text{Cl}_2$ (CCOC) was recently reported⁹. Subsequently, it was found that the high energy kink also exists in doped cases, making it omnipresent at all dopings^{10,11}. Existence of the high energy kink reveals that there may be another energy scale from the many-body interactions in HTSCs. It is thus important to find the physics in this high energy scale.

One can extract from the data the information on the many-body interactions through the self energy analysis. Conventionally, the self energy analysis is done by extracting the dispersion and peak width from the momentum distribution curves (MDCs)¹. However, there are underlying assumptions for the analysis to be valid. First of all, ARPES peaks should be sharp enough to be quasiparticle-like. Secondly, the bare band dispersion should be quite linear within the energy range of interest so that one can “guess” the bare band dispersion. Unfortunately, none of these are valid assumptions in the analysis of ARPES spectral function from CCOC: The peaks are too broad to be considered as quasi-particle peaks^{12,13} and there is an inherent confusion regarding what should be considered as the original bare band as CCOC is a Mott insulator. Similar limitations also apply

to the recently found high energy kinks in HTSCs^{10,11}. However, the lack of quasiparticles should not be confused with a lack of physics. For example, in Luttinger liquids, where Fermi liquid quasiparticles do not exist, ARPES has provided detailed information on the excitation spectrum¹⁴.

It is therefore necessary to develop a method to extract the self energy from non-quasi particle ARPES spectral functions. In fact, there was an earlier attempt to obtain the self energy through a Hilbert transformation with the assumption of particle-hole symmetry¹⁵. This method however is not applicable to systems without particle-hole symmetry (for example, CCOC¹⁶). Here we propose to use the self energy defined for the electron *removal* Green's function. Even though different, it bares similar characters of the usual self energy and its imaginary part is found to appropriately represent the width of the spectral feature. Moreover, we developed a method to extract the self energy from a general ARPES spectrum from a single band system. It can thus be used to for spectral functions with broad spectral features. We believe our analysis method provides a new way to examine the underlying physics from photoemission spectral functions.

II. METHODOLOGY

The full Green's function for a single band system at 0 K can be written as

$$\begin{aligned} G^{Full}(\mathbf{k}, \omega) &= \sum_n \left[\frac{|\langle n | c_k | 0 \rangle|^2}{\omega - E_n + i\delta} + \frac{|\langle n | c_k^\dagger | 0 \rangle|^2}{\omega - E_n + i\delta} \right] \\ &= \frac{1}{\omega - \varepsilon_k - \Sigma^{Full}(\mathbf{k}, \omega)} \end{aligned} \quad (1)$$

where ε_k and $\Sigma^{Full}(\mathbf{k}, \omega)$ are the bare band and self energy, respectively. The chemical potential μ is set to zero for convenience. Note that due to the sum rule $\sum_n \{|\langle n | c_k | 0 \rangle|^2 + |\langle n | c_k^\dagger | 0 \rangle|^2\} = 1$, the asymptotic behav-

ior ($\omega \rightarrow \infty$) of G^{Full} is $1/\omega$. This makes the self energy non-divergent when $\omega \rightarrow \pm\infty$. In addition, the self energy is analytic in the positive complex plane, and as a consequence the real and imaginary parts of the self energy are Hilbert transforms of each other¹⁷. The Green's function defined in this way ("full Green's function") is thought to represent electron addition or removal processes and the self energy holds the information on the interaction.

The full Green's function in the above equation however includes not only electron removal but also electron addition process for which we do not have information. Our goal is to obtain the self energy from a general spectral function with as few assumptions as possible. Therefore, we attempt to look at the self energy for the electron removal Green's function which should best describe the ARPES process and is defined as

$$\begin{aligned} G^{ER}(\mathbf{k}, \omega) &= \sum_n \frac{|\langle n | c_k | 0 \rangle|^2}{\omega - E_n + i\delta} \\ &= \frac{n_k}{\omega - \varepsilon_k - \Sigma^{ER}(\mathbf{k}, \omega)} \end{aligned} \quad (2)$$

or

$$\begin{aligned} \Sigma^{ER}(\mathbf{k}, \omega) &= \omega - \varepsilon_k - \frac{n_k}{G^{ER}(\mathbf{k}, \omega)} \\ &= \omega - \varepsilon_k - \frac{n_k}{\sum_n \frac{|\langle n | c_k | 0 \rangle|^2}{\omega - E_n + i\delta}} \end{aligned} \quad (3)$$

where $n_k = \sum_n |\langle n | c_k | 0 \rangle|^2 = \int A^{ER}(\mathbf{k}, \omega) d\omega$ and $A^{ER}(\mathbf{k}, \omega)$ is the electron removal spectral function (the superscript ER stands for "electron removal"). Another difference is that ε_k may not be the bare band dispersion as will be discussed later. The asymptotic behavior of G is now n_k/ω and with the definition given in equation (2), the real and imaginary parts of the electron removal self energy ($\text{Re}\Sigma^{ER}$ and $\text{Im}\Sigma^{ER}$, respectively) are again related through Hilbert transforms.

To obtain the electron removal self energy Σ^{ER} , we use the fact that the measured ARPES spectrum is proportional to the electron removal spectral function, that is,

$$\begin{aligned} I_{ARPES}(\mathbf{k}, \omega) \equiv I &= |M(\mathbf{k})|^2 A^{ER}(\mathbf{k}, \omega) \\ &= -\frac{|M(\mathbf{k})|^2}{\pi} \text{Im}G^{ER}(\mathbf{k}, \omega) \end{aligned} \quad (4)$$

where I_{ARPES} and $M(\mathbf{k})$ are the measured ARPES spectrum and matrix element, respectively. Here, the ω dependence of the matrix element $M(\mathbf{k})$ is ignored as usual. Note that the Fermi function is missing as we deal with the electron *removal* Green's and spectral functions. The real and imaginary parts of the electron removal Green's function are, as is the case for G^{Full} , Hilbert transforms of each other, $\text{Re}G^{ER} = H(\text{Im}G^{ER})$ where $H()$ represents the Hilbert transformation. Then the combination of equations (3) and (4) gives¹⁵,

$$\text{Re}\Sigma^{ER} = \omega - \varepsilon_k - C(\mathbf{k}) \frac{H(I)}{H(I)^2 + I^2} \quad (5)$$

$$\text{Im}\Sigma^{ER} = C(\mathbf{k}) \frac{I}{H(I)^2 + I^2} \quad (6)$$

where ε_k and $C(\mathbf{k})$ are the bare band and $-n_k|M(\mathbf{k})|^2/\pi$, respectively.

The only remaining task to get Σ is to determine $C(\mathbf{k})$ and ε_k . We can obtain $C(\mathbf{k})$ by integrating both sides of equation (4).

$$\begin{aligned} \int I_{ARPES}(\mathbf{k}, \omega) d\omega &= -\frac{\pi C(\mathbf{k})}{n_k} \int A^{ER}(\mathbf{k}, \omega) d\omega \\ &= -\frac{\pi C(\mathbf{k})}{n_k} n_k = -\pi C(\mathbf{k}) \end{aligned} \quad (7)$$

To define ε_k , we enforce the standard relationship $\text{Re}\Sigma^{ER} = H(\text{Im}\Sigma^{ER})$. For this relationship to hold, $\Sigma^{ER}(\mathbf{k}, \omega) \rightarrow 0$ as $\omega \rightarrow \pm\infty$. By expanding the last term in equation (3) in terms of $1/\omega$ for $\omega \rightarrow \pm\infty$, we get

$$\begin{aligned} \Sigma^{ER} &= \omega - \varepsilon_k - \frac{n_k \omega}{\sum_n \frac{|\langle n | c_k | 0 \rangle|^2}{1 - E_n/\omega}} \\ &\approx \omega - \varepsilon_k - \frac{n_k \omega}{\sum_n |\langle n | c_k | 0 \rangle|^2 + \sum_n |\langle n | c_k | 0 \rangle|^2 E_n/\omega}. \end{aligned} \quad (8)$$

Using $\sum_n |\langle n | c_k | 0 \rangle|^2 = n_k$ and $\sum_n |\langle n | c_k | 0 \rangle|^2 E_n/n_k \equiv \bar{\varepsilon}_k$, Σ^{ER} becomes

$$\Sigma^{ER} = \omega - \varepsilon_k - \frac{n_k \omega}{n_k + n_k \bar{\varepsilon}_k/\omega} \approx \bar{\varepsilon}_k - \varepsilon_k. \quad (9)$$

Since $\Sigma^{ER}(\mathbf{k}, \omega) \rightarrow 0$ as $\omega \rightarrow \pm\infty$, we set $\varepsilon_k = \bar{\varepsilon}_k$ and thus we have

$$\varepsilon_k = \frac{\int \omega A^{ER}(\mathbf{k}, \omega) d\omega}{\int A^{ER}(\mathbf{k}, \omega) d\omega} = \frac{\int \omega I_{ARPES}(\mathbf{k}, \omega) d\omega}{\int I_{ARPES}(\mathbf{k}, \omega) d\omega}. \quad (10)$$

That is, ε_k is the center of gravity of the spectral function but may not be the true bare band.

We rationalize this definition of ε_k from the knowledge that $\bar{\varepsilon}_k = \varepsilon_k$, the bare band value, independent of the strength of interactions in the limit $n_k \rightarrow 1$ ¹⁸. Alternatively, ε_k could have been chosen differently such as the true bare band value of the original non-interacting problem but it will only shift $\text{Re}\Sigma^{ER}$ determined here by a constant. In that case, the relationship between $\text{Re}\Sigma^{ER}$ and $\text{Im}\Sigma^{ER}$ would be modified to $\text{Re}\Sigma^{ER} = H(\text{Im}\Sigma^{ER}) + \bar{\varepsilon}_k - \varepsilon_k$. We note then that $\text{Re}\Sigma^{ER}$ goes to a finite value of $\bar{\varepsilon}_k - \varepsilon_k$ as $\omega \rightarrow \pm\infty$ (similarly $\text{Re}\Sigma^{Full}$ asymptotically goes to the Hartree-Fock value). Using this expression we can see that the parameter ε_k drops out and that the imaginary part of the self energy remains uniquely determined independent of our choice of ε_k .

III. RESULTS

In applying the newly developed method to the ARPES data, one has to consider other aspects of the

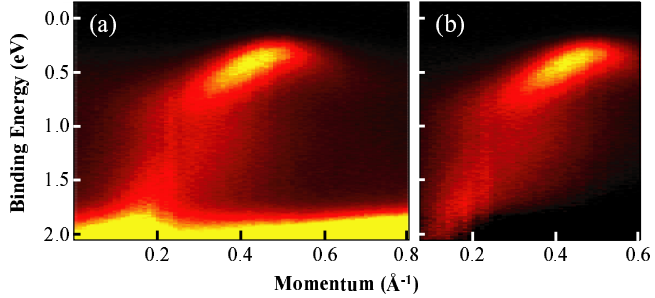


FIG. 1: (Color online) (a) Published ARPES data from CCOC along the $(0,0)$ to (π,π) cut in Ref 8. (b) Same data after background is removed. Data is presented for a smaller momentum window where peaks are reasonably strong.

experimental data such as experimental resolution and thermal broadening. In that respect, CCOC can be an ideal system to test the method: The experimental resolution and thermal broadening are much smaller than the width of the characteristic features of CCOC and thus can be ignored. This provides an extra motivation for this study. For the experimental data, we use the published CCOC data along the $(0,0)$ to (π,π) cut shown in Fig. 1(a)⁹.

Before we apply the procedure to extract Σ^{ER} , we also have to subtract the background intensity from the data. This is because the background intensity is from a process that can not be described by the Green's function in equation (2). In our case, subtracting the background so that $A^{ER}(\mathbf{k},\omega) \rightarrow 0$ as $\omega \rightarrow \pm\infty$ is a necessary condition for $\text{Re}\Sigma^{ER}$ and $\text{Im}\Sigma^{ER}$ to be Hilbert transforms of each other. The background intensity is also casually subtracted in other methods, either naturally by fitting the MDCs¹ or enforcing it¹⁵. There are a number of potential ways to subtract the background, among which we may consider the following two. The first one is subtracting the Shirley background^{19,20}. The other is subtracting the intensity of the unoccupied \mathbf{k} states (approximately beyond $k = 0.7\text{\AA}$ in Fig. 1(a)), that is, the MDC background assuming that it is from the momentum independent background intensity. We show the result extracted by using the latter method in Fig. 1(b). However, the final results are similar independent of the background subtraction method.

In panels (a) and (b) of Fig. 2, we show $\text{Re}\Sigma^{ER}$ and $\text{Im}\Sigma^{ER}$ obtained by applying the procedure discussed above. Note that while $\text{Re}\Sigma^{ER}$ can be negative, $-\text{Im}\Sigma^{ER}$ is always positive. The most notable aspect of the data is that overall k dependence for both $\text{Re}\Sigma^{ER}$ and $\text{Im}\Sigma^{ER}$ is weak. This is very striking considering the fact that the dispersion of the spectral features is very strong. The momentum independence of the self energy which has been casually assumed^{1,8,22,23,24,25} is indeed seen in the data. The momentum independence could further be tested for our systems. Yet, we still see some momentum dependence of the self energy, especially at the low energy side. Therefore, for the accurate measure of the

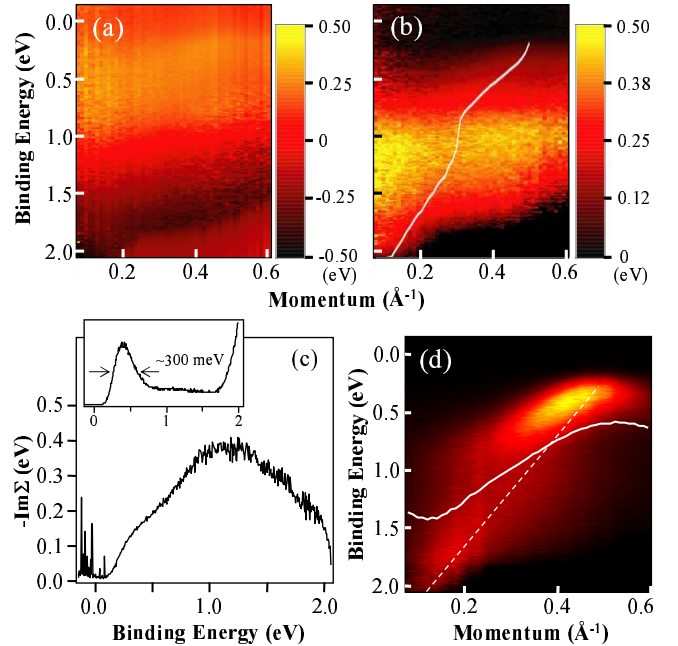


FIG. 2: (Color online) (a) $\text{Re}\Sigma^{ER}$ extracted from the data in Fig. 1(a). The energy scale is coded in the color scales on the right. (b) $-\text{Im}\Sigma^{ER}$. The line is the dispersion extracted from fitting the MDCs. (c) $-\text{Im}\Sigma^{ER}$ along the MDC dispersion in panel (b). The inset shows the EDC from the k point where the spectrum is the peakiest. The full width at half maximum of the peak is about 300 meV. (d) Comparison of the ε_k (solid line), and the MDC dispersion at the high binding energy side and its extrapolation to the low energy side (dashed line). ARPES data is shown in the background for the comparison purpose.

self energy, it is important to have the self energy in the full $\mathbf{k}-\omega$ space as is the case for our method.

The potential importance of the above observation can not be understated. The largest shortcoming of dynamical mean field theory (DMFT) is that momentum independence of the self energy must be assumed (some momentum dependence can be added back in with cluster calculations, but this is computationally very expensive)^{26,27}. While experimental limitations forced us to make a few assumptions such as the background subtraction, our results are encouraging that the momentum independent self energy assumption made in DMFT calculations of the cuprates are valid. To our knowledge, this is the first experimental attempt to prove the validity of this assumption.

Looking at $\text{Im}\Sigma^{ER}$ plotted in panel (b), one may wonder about the validity of the result near the gap region as $\text{Im}\Sigma^{ER}$ is zero while it is known that $\text{Im}\Sigma^{Full}$ diverges near the gap region²¹. The divergence of $\text{Im}\Sigma^{Full}$ near the gap is due to the fact that multiple poles of G^{Full} (or two peak structure in $A^{Full}(\mathbf{k},\omega)$) are attempted to be described by a single pole with a self energy. However, by using only the occupied part, A^{ER} effectively becomes a single peak spectral function. As $\text{Im}\Sigma^{Full}$ does

not diverge for a single peak spectral function, $\text{Im}\Sigma^{ER}$ calculated from an effective single peak does not necessarily diverge even though CCOC is an insulator. This issue will be discussed again with simulations presented in Fig. 3.

In the conventional method of fitting MDCs and converting the MDC widths to EDC widths¹, one estimates the width, thus $\text{Im}\Sigma^{ER}$, at the peak positions. We present the result in a similar fashion by plotting $\text{Im}\Sigma^{ER}$ along the dispersion. This provides the most accurate estimate of Σ^{ER} of the feature because of the possible momentum dependence discussed above. In Fig. 2(c), we plot $-\text{Im}\Sigma^{ER}$ along the MDC dispersion shown in panel (b). At this point, it is worth checking the validity of the new result. One way of doing so is to compare the $\text{Im}\Sigma^{ER}$ obtained by the new method with the value from a conventional method (if such a method can be applied). In the case of CCOC, a conventional way of measuring the half width of a quasiparticle-like peak may be applicable only to the features with the lowest binding energy. In the inset, we plot the EDC of the feature that has the lowest binding energy of 0.4 eV, hence is sharpest. The half width of the feature is about 150 meV. $\text{Im}\Sigma^{ER}$ at 0.4 eV indeed shows a similar value. This fact gives us confidence in the new method.

Looking at $\text{Im}\Sigma^{ER}$ curve in panel (c), one sees “bends” at about 0.3 and 1 eV binding energies. 0.3 eV is where the spectral weight of the lowest binding energy feature starts as can be seen from Fig. 1(a). Therefore, the bend at 0.3 eV may not mean any coupling energy. Meanwhile the bend at 1 eV is in the middle of the dispersion. Interestingly, 1 eV binding energy is where the kink-like dispersion appears to have “bosonic mode” coupling. When the kink-like feature from CCOC was first reported⁹, the most obvious problem with the interpretation of it in terms of bosonic mode coupling was how an insulator can have bosonic mode coupling. Strictly speaking, an insulator can have bosonic mode coupling and should display kink-like features even though the effect would be small²⁸. Even though it does not show the origin, our analysis firmly shows that $\text{Im}\Sigma^{ER}$ behaves as if there is a bosonic mode coupling at 1 eV (or 0.6 eV from the top of the band). This value is comparable to the energy found in doped HTSCs^{10,11}.

In Fig. 2(d), we plot the MDC dispersion of the high energy features and its extrapolation as the dashed line. This has a strong resemblance to the LDA band and may serve as the bare band⁹. Also plotted in the panel is the ε_k obtained by calculating the center of the gravity of the spectral function. In comparing the two, one sees very little resemblance between them. The deviation of ε_k from the bare band near $k = 0.5\text{\AA}^{-1}$ (where $n_k \neq 1$) is from the reason discussed above. Meanwhile, we believe the difference near $k = 0$, where we expect n_k to be closer to 1, is from the fact that we cut out the spectral weight at high binding energies under the main valence band²⁹ during the background subtraction.

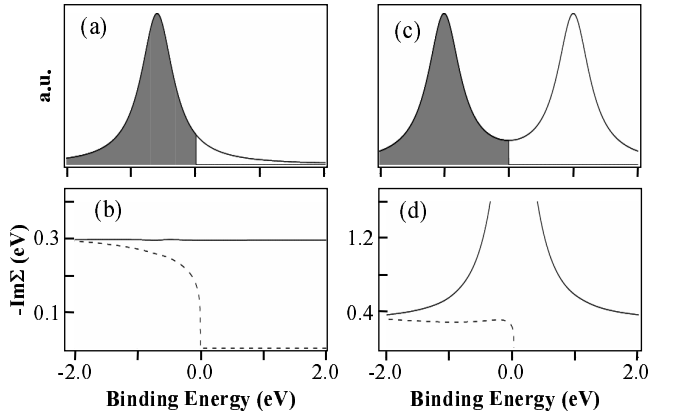


FIG. 3: (a) A Lorentzian peak with an width of 0.3 eV representing a spectral function $A^{Full}(\mathbf{k}, \omega)$. The filled area below the Fermi energy represents the electron removal spectral function $A^{ER}(\mathbf{k}, \omega)$. (b) $-\text{Im}\Sigma^{Full}$ (solid) and $-\text{Im}\Sigma^{ER}$ (dashed) of the spectral functions in (a). (c) Two Lorentzian peaks of 0.3 eV width, simulating a situation where there is a gap at the Fermi energy. The filled area again represents $A_{ER}^{Full}(\mathbf{k}, \omega)$ on the red solid line (blue solid line). (d) $-\text{Im}\Sigma^{Full}$ (solid) and $-\text{Im}\Sigma^{ER}$ (dashed) of the spectral functions in (c).

An important question is whether the self energy defined only for the electron removal process is meaningful. We argue that it still bares useful information. First of all, the self energy defined in this way is identical to the usual Σ^{Full} when $n_k = 1$. This is important because for most of the cases one analyzes the self energy for the occupied parts of the momentum space where $n_k \approx 1$. In addition, we find that $\text{Im}\Sigma^{ER}$ measures the “width” of spectral function fairly well in various cases as illustrated below. Lastly, on the practical side, the method can also be applied when the dispersion is flat and therefore MDCs can not be obtained. This is very useful when the dispersion does not cross the Fermi energy as in insulators. To discuss if $\text{Im}\Sigma^{ER}$ indeed measures the width of the occupied part of a spectral function well, we use numerical simulations as illustrated in Fig. 3. The first case, shown in panel (a), is when the spectral weight is truncated by the Fermi function. From the results plotted in panel (b), we find that $\text{Im}\Sigma^{ER}$ still measures the width of the peak fairly well below the Fermi energy. We may also discuss cases where there is a gap at the Fermi energy and the spectral function splits into two due to, for example, charge density wave or Mott transition. To simulate such cases, we use two Lorentzian peaks as shown in panel (c). From the self energies plotted in panel (d), we find that $\text{Im}\Sigma^{ER}$ is very close to the Lorentzian peak width while $\text{Im}\Sigma^{Full}$ has a large value near $\omega=0$. These numerical simulation results support the assertion that $\text{Im}\Sigma^{ER}$ measures the width of the occupied part of a spectral feature. The case illustrated in panels (c) and (d) is also relevant to the discussion on the behavior of the self energies in the gap region. While $\text{Im}\Sigma^{Full}$ has a large value at $\omega=0$, $\text{Im}\Sigma^{ER}$ stays at a finite value close

to the peak width.

Our method, as it is, may not be used for multi-band systems. This is due to the fact that states from different bands may have different matrix element $M(\mathbf{k})$. However, our scheme in principle can be extended to multi-band systems even though it is more difficult. If it can be extended to multi-band system, our method will find far more applicability and usefulness in the analysis of self energies of many-body systems. This is at the present left for the future work.

IV. CONCLUSION

In conclusion, we propose using the electron removal self energy which is found to represent the spectral width very well. The method has the advantage that one can easily extract the self energy from a spectral function

with arbitrary shape, allowing us to avoid making inappropriate assumptions. Application of the new method to experimental data from CCOC reveals momentum independence of $\Sigma(\mathbf{k},\omega)$ which has been an assumption in the conventional analysis. We expect this new method to be useful in strongly correlated systems where spectral features are often quite broad.

Acknowledgments

Authors would like to thank B. J. Kim for a key suggestions in programming and W. Meevasana, Jun Won Rhim and Jung Hoon Han for helpful discussions. This work is supported by the KOSEF through CSCMR and by the KICOS through a grant provided by MOST in M60602000008-06E0200-00800. Work at Los Alamos was performed under the auspices of US DOE.

-
- ^{*} Electronic address: cykim@phya.yonsei.ac.kr
- ¹ B. A. McDougall, T. Balasubramanian, and E. Jensen, Phys. Rev. B **51**, 13891 (1995).
 - ² M. Hengsberger, D. Purdie, P. Segovia, M. Garnier, and Y. Baer, Phys. Rev. Lett. **83**, 592 (1999).
 - ³ T. Valla, A. V. Fedrov, P. D. Johnson, and S. L. Hulbert, Phys. Rev. Lett. **83**, 2085 (1999)
 - ⁴ P.V. Bogdanov, A. Lanzara, S.A. Kellar, X.J. Zhou, E.D. Lu, W.J. Zheng, G. Gu, J.-I. Shimoyama, K. Kishio, H. Ikeda, R. Yoshizaki, Z. Hussain, and Z.-X. Shen, Phys. Rev. Lett. **85**, 2581 (2000).
 - ⁵ A. Lanzara, P. V. Bogdanov, X. J. Zhou, S. A. Kellar, D. L. Feng, E. D. Lu, T. Yoshida, H. Eisaki, A. Fujimori, K. Kishio, J.-I. Shinoyama, T. Noda, S. Uchida, Z. Hussain, and Z.-X. Shen, Nature (London) **412**, 510 (2001).
 - ⁶ A. Kaminski, M. Randeria, J. C. Campuzano, M. R. Norman, H. Fretwell, J. Mesot, T. Sato, T. Takahashi, and K. Kadowaki Phys. Rev. Lett. **86**, 1070 (2001).
 - ⁷ A. D. Gromk, A. V. Fedorov, Y.-D. Chuang, J. D. Koralek, Y. Aiura, Y. Yamaguchi, K. Oka, Yoichi Ando, and D. S. Dessau, Phys. Rev. B **68**, 174520 (2003).
 - ⁸ W. Meevasana, N. J. C. Ingle, D. H. Lu, J. R. Shi, F. Baumberger, K. M. Shen, W. S. Lee, T. Cuk, H. Eisaki, T. P. Devereaux, N. Nagaosa, J. Zaanen, and Z.-X. Shen, Phys. Rev. Lett. **96**, 157003 (2006).
 - ⁹ F. Ronning, K. M. Shen, N. P. Armitage, A. Damascelli, D. H. Lu, Z.-X. Shen, L. L. Miller, and C. Kim, Phys. Rev. B **71**, 094518 (2005).
 - ¹⁰ B. P. Xie, K. Yang, D. W. Shen, J. F. Zhao, H. W. Ou, J. Wei, S. Y. Gu, M. Arita, S. Qiao, H. Namatame, M. Tanaguchi, N. Kaneko, H. Eisaki, Z. Q. Yang, and D. L. Feng, Phys. Rev. Lett. **98**, 147001 (2007).
 - ¹¹ J. Graf, G.-H. Gweon, K. McElroy, S. Y. Zhou, C. Jozwiak, E. Rotenberg, A. Bill, T. Sasagawa, H. Eisaki, S. Uchida, H. Takagi, D.-H. Lee, and A. Lanzara, Phys. Rev. Lett. **98**, 067004 (2007).
 - ¹² C. Kim, F. Ronning, A. Damascelli, D. L. Feng, Z.-X. Shen, B. O. Wells, Y. J. Kim, R. J. Birgeneau, M. A. Kastner, L. L. Miller, H. Eisaki and S. Uchida, Phys. Rev. B **65**, 174516 (2002).
 - ¹³ K. M. Shen, F. Ronning, W. Meevasana, D. H. Lu, N. J. C. Ingle, F. Baumberger, W. S. Lee, L. L. Miller, Y. Kohsaka, M. Azuma, M. Takano, H. Takagi, and Z.-X. Shen, Phys. Rev. B **75**, 075115 (2005).
 - ¹⁴ B. J. Kim, H. Koh, E. Rotenberg, S.-J. Oh, H. Eisaki, N. Motoyama, S. Uchida, T. Tohyama, S. Maekawa, Z.-X. Shen and C. Kim, Nat. Phys. **2**, 397 (2006).
 - ¹⁵ M. R. Norman, H. Ding, H. Fretwell, M. Randeria, J. C. Campuzano, Phys. Rev. B **60**, 7585 (1999).
 - ¹⁶ M. Z. Hasan, E. D. Isaacs, Z.-X. Shen, L.L. Miller, K. Tsutsui, T. Tohyama, and S. Maekawa, Science **288**, 1811 (2000).
 - ¹⁷ J. M. Luttinger, Phys. Rev. **121**, 942 (1961).
 - ¹⁸ D. C. Langreth, Phys. Rev. B **1**, 471 (1970).
 - ¹⁹ D. A. Shirley, Phys. Rev. B **5**, 4709 (1972).
 - ²⁰ S. Hüfner, *Photoelectron spectroscopy : principles and application*, Oxford University, New York : Springer-Verlag, 1995.
 - ²¹ R. Bulla, T. A. Costi and D. Vollhardt, Phys. Rev. B **64**, 045103 (2001).
 - ²² Anil Khurana, Phys. Rev. B **40**, 4316 (1989); P. W. Anderson, Princeton University lecture notes on stononly interacting fermions (unpublished).
 - ²³ M. Eschrig and M. R. Norman, Phys. Rev. B **67**, 144503 (2003).
 - ²⁴ A. A. Kordyuk, S. V. Borisenko, A. Koitzsch, J. Fink, M. Knupfer, and H. Berger, Phys. Rev. B **71**, 214513 (2005).
 - ²⁵ A. A. Kordyuk, S.V. Borisenko, V. B. Zabolotnyy, J. Geck, M. Knupfer, J. Fink, B. Buchner, C. T. Lin, B. Keimer, H. Berger, A.V. Pan, Seiki Komiya, and Yoichi Ando, Phys. Rev. Lett. **97**, 017002 (2006).
 - ²⁶ A. Georges, G. Kotliar, W. Krauth and M. J. Rozenberg, Rev. Mod. Phys. **68**, 13 (2006).
 - ²⁷ G. Kotliar, S. Y. Savrasov, K. Haule, V. S. Oudovenko, O. Parcollet, C. A. Marianetti, Rev. Mod. Phys. **78**, 865 (2006).
 - ²⁸ C. S. Leem, B. J. Kim, Chul Kim, S. R. Park, T. Ohta, E. Rotenberg, H.-D. Kim, M. K. Kim, H. J. Choi, and C. Kim, unpublished.
 - ²⁹ H. Eskes and R. Eder, Phys. Rev. B **54**, R14226 (1996).